CrossMark

ORIGINAL ARTICLE

Spatiotemporal dynamics of arable land in the Nanjing metropolitan region, China

Guilin Liu · Luocheng Zhang · Hailin You

Abstract Arable land change trends, namely stable arable land, change into arable land, change into non-arable land, stable non-arable land and ephemeral arable land were subsequently categorized from the temporal trajectories of arable land changes. To deeper understand the landscape change patterns consequent from arable land use, three metrics at class level were employed. Arable land, in general, decreased by 57.24 % during 1985–2010. The change trajectory from arable to non-arable land was consistent with urban expansion. Change trajectory from arable into non-arable land was mainly located in Jiangning District while stable arable land coverage was high in Liuhe District. Stable arable land was mainly dominant in locations away from the city center. Trends in stable non-arable land, however, had a completely opposite trajectory to that of arable into non-arable land. About 59.26 % change into non-arable land was located within 10–15 km buffers and was more dramatic than other trajectories and characterized with high fragmentation. Rural labor migration, economic development, policies and urban expansion were the major driving force associated with the observed arable land changes.

Keywords Temporal trajectory analysis · Arable land · Landscape metrics · Driving forces · Nanjing metropolitan region

G. Liu · L. Zhang (✉)
State Key Laboratory of Lake Science and Environment,
Nanjing Institute of Geography and Limnology, Chinese
Academy of Sciences, Nanjing 210008, China
e-mail: lchzhang@niglas.ac.cn

G. Liu
e-mail: guilinshiwo@163.com

G. Liu
Department of Environmental Remote Sensing and
Geoinformatics, University of Trier, 54286 Trier, Germany

G. Liu
University of Chinese Academy of Sciences,
Beijing 100049, China

H. You
Research Center of Poyang Lake, Jiangxi Academy of Sciences,
Nanchang 330096, China

Introduction

Land use and land cover change, proposed by the International Geosphere-Biosphere Program (IGBP) and International Human Dimensions Program on Global Environmental Change (IHDP), is not only the core of land changes science but also the intuitive performance of global changes (Turner et al. 1995). Arable land plays a critical role in rural livelihood sustainability and development, especially in developing countries where agriculture is the mainstay economy. However, there is always a conflict of land use interests between arable land and economic developments as reflected by the loss of arable land to economic developments and urbanization (Long et al. 2009). Therefore, arable land use change reflects the response of a society or the human-land relationship to agricultural production and socio-economic development (Feng et al. 2011).

Land use and land cover change analysis approaches have considerably developed in alignment with the development of remote sensing technology (Liu et al. 2005a, 2014a; Turner et al. 2003), a fact that has allowed a better understanding of the change processes and hence better management. Land use/cover change methods based on

Springer

remote sensing are mainly divided into two categories: bi-temporal change detection and temporal trajectory analysis (Coppin et al. 2004). The former usually uses remote sensing data of more than two epochs to analyze the land use spatial and temporal dynamics (Zhou et al. 2008a). A limitation of bi-temporal change detection method is that it is not possible to do a detailed land use change of the processes and trends. Temporal trajectory land cover change defined as successional process of land cover types during more than two epochs (Lambin 1997) was proposed to overcome the shortcomings of the bi-temporal change detection method. This approach has been successfully applied to highlight land cover changes and their driving forces (Lu et al. 2004; Kuemmerle et al. 2009; Zhou et al. 2008b; Wang et al. 2012).

Nanjing has experienced rapid and high economic developments and exacerbated urban expansion. Thus, concerns on the arable land spatial temporal dynamics are obvious. However, previous studies on land use of Nanjing metropolitan region are rare. So, what are the detailed change processes and trend in arable land during 1985–2010? This paper applies the temporal trajectory analysis approach to evaluate the spatial–temporal dynamics of arable lands in Nanjing metropolitan region. Thus, this study aimed specifically to: (1) extract arable land and model change trajectories based on Landsat data; (2) analyze spatial pattern of arable land change trajectories coupling with landscape metrics; and (3) illustrate the relationship between arable land change and human-induced factors.

Data and methodology

Study area

Nanjing is the capital of Jiangu and is located in the southwest of Jiangsu Province (Fig. 1). Nanjing metropolitan region includes Jiangning, Pukou, Liuhe District and Jiangnan Eight Districts (including Jianye, Gulou, Baixia, Xuanwu, Xiaguan, Qinhuai, Yuhuatai and Qixia). It holds 7.4 million permanent residents and covers administrative areas of 6,515 km^2 (Ouyang et al. 2012). Nanjing has a humid subtropical climate and is under the influence of the East Asia Monsoon (Shi et al. 2012). It experiences a mean annual temperature of 15.7 °C and an average precipitation is 1,106.5 mm (Xu et al. 2010).
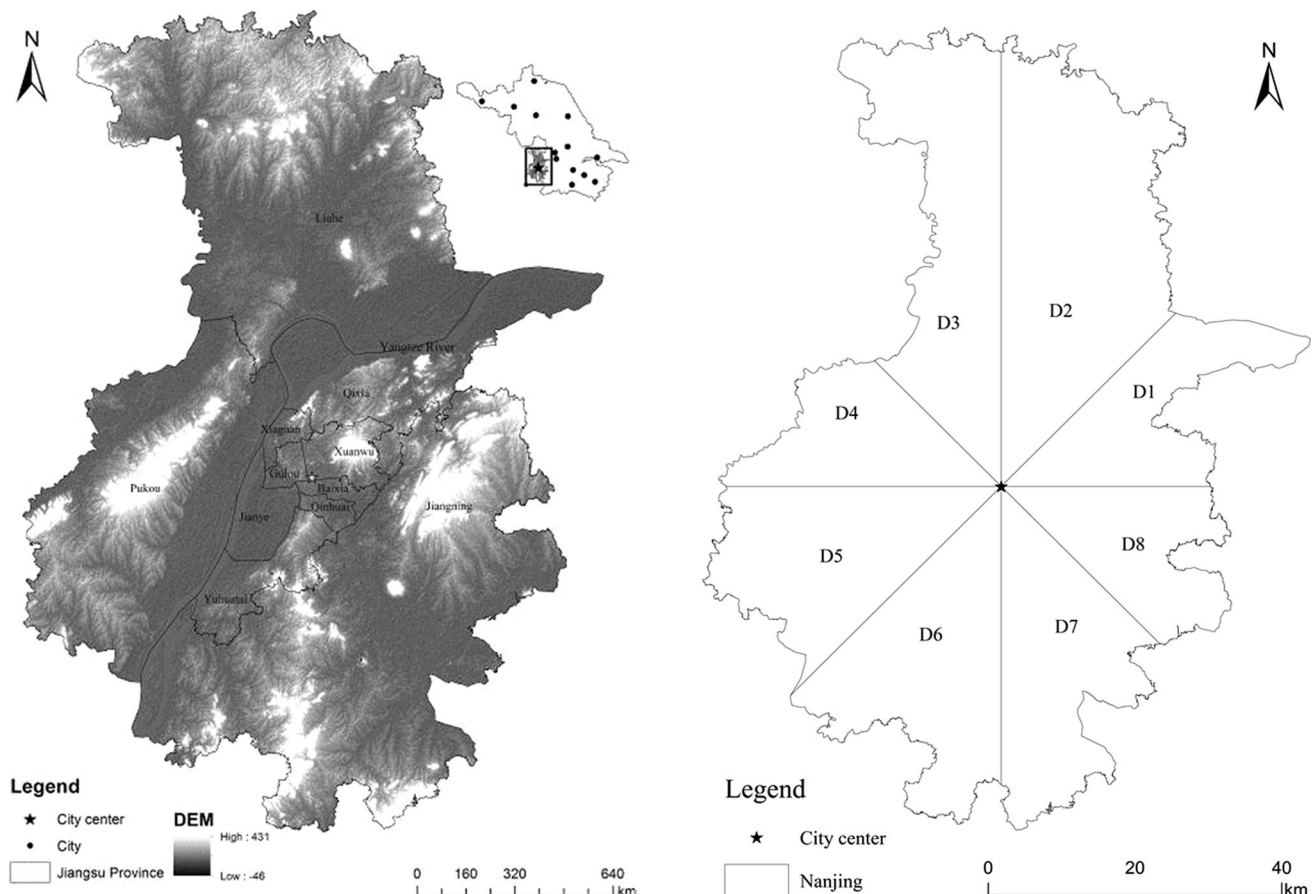
Fig. 1 The location of Nanjing metropolitan region and the distribution of its directions

Urban expansion of this region is rapid, especially within the metropolitan due to urban developments. This in turn has resulted in loss in arable land. Changes in arable land are mainly located in the urban fringe zone of Nanjing. Therefore, this paper selected Nanjing metropolitan region as study area due to the extended urbanization in the region.

Data source

Landsat 5 Multispectral Scanner (MSS) and Thematic Mapper (TM) remotely sensed imageries covering Nanjing metropolitan region were acquired from US Geological Survey from 1985 to 2010. Optimum imageries were selected based on crop planting calendar, and presence of no cloud cover (Table 1). Land cover samples were obtained using handheld GPS while the socio-economic data were acquired from Nanjing Statistical Yearbook.

Remote sensing images processing and classification

The ground control points from field work were used to rectify Landsat remotely sensed imageries from 1985 to 2010. Radiometric calibration was used to transform digital values into reflectance values (Markham and Barker 1987; Price 1987; Moran et al. 1992; Liu et al. 2014b). The Landsat MSS image was upscale by resampling it into 30 m.

Five land cover categories, namely, arable land, forest, water body, built-up land and unused land were developed based on the classification criteria of State Bureau of Land Administration and Chinese Academy of Sciences (Liu et al. 2005b, 2014c). Maximum likelihood classification method was employed to classify the images. Finally, the land use classification results were reclassified into arable and non-arable land maps.

Modelling of arable land change trajectories

Land cover change temporal trajectory was defined as chronological arrangement of land cover types. Arable and non-arable land was coded A and O, respectively. Arable

land trajectories were calculated using formula 1 as follows:

$$N_{\text{trac}} = \sum_{i=1}^{n} \left(2^i \times A_i \right) \tag{1}$$

where N_{trac} is the number of arable land change trajectories, n is epoch, A_i is the arable land map in epoch i.

In this article, change trajectories were categorized as: stable arable land, stable non-arable land, change into arable land, change into non-arable land and ephemeral arable land (Table 2).

Spatial analysis of arable land change trajectories

Arable land change trajectory analysis in various directions

To reveal spatial variation of arable land changes in different directions, the study area was divided into eight equal-angle sectors around city center (Fig. 1). The directions were numbered counterclockwise as D1–D8 representing the eight directions as follows: D1 "East–Northeast (0°–45°)", D2 "Northeast–North (45°–90°)", D3 "North–Northwest (90°–135°)", D4 "Northwest–West (135°–180°)", D5 "West–Southwest (180°–225°)", D6 "Southwest–South (225°–270°)", D7 "South–Southeast (270°–315°)", D8 "Southeast–East (315°–360°)".

Arable land change trajectory analysis in various counties

To analyze the variations of arable land changes in Nanjing metropolitan, the analysis was performed as per the administrative counties.

Arable land change trajectory analysis in various buffers

To reveal spatial variation along the urban–rural gradient, the buffers of 5, 10, 15, 20, 25 and 30 km from the city

Table 1 Path/row and acquiring date of remotely sensed imageries

Satellite	Sensor	Path/row	Resolution (m)	Acquisition date
Landsat 5	MSS	129/37, 129/38	79	1985_04_24
Landsat 5	TM	120/37, 120/38	30	1990_10_15
Landsat 5	TM	120/37, 120/38	30	1995_10_13
Landsat 5	TM	120/37, 120/38	30	2000_05_03
Landsat 5	TM	120/37, 120/38	30	2007_07_26
Landsat 5	TM	120/37, 120/38	30	2010_08_19

Table 2 Change trajectories' categories and their definitions

Types	Typical code	Definition
Stable arable land	AAAAAA	Arable land remained arable in the six epochs
Stable non-arable land	OOOOOO	Non-arable land remained non-arable in the six epochs
Change into arable land	OOOAAA	Change trend from non-arable land to arable land
Change into non-arable land	AAAOOO	Degradation and loss trends of arable land
Ephemeral arable land	AOAOAO	Irregular arable land change trend

Table 3 Description of landscape pattern metrics used in this paper

Landscape metrics	Algorithm	Range
Number of patches (NP)	$NP = n_i$	$NP \geq 1$, without limit
Interspersion and Juxtaposition (IJI)	$IJI = \dfrac{-\sum\limits_{k=1}^{m}\left[\left(\dfrac{e_{ik}}{\sum\limits_{k=1}^{m} e_{ik}}\right)\ln\left(\dfrac{e_{ik}}{\sum\limits_{k=1}^{m} e_{ik}}\right)\right]}{\ln(m-1)} \times 100$	$0 < IJI \leq 100$
Percentage of landscape (PLAND)	$PLAND = 100 \times \sum\limits_{j=1}^{n} a_{ij}\Big/ A$	$0 < PLAND \leq 100$

m total number of types in the area, a_{ij} area of the jth patch belong to the ith landscape, e_{ik} total length of edge in landscape between classes i and k, n_i number of patches in the landscape of patch type (class) i

center were developed using buffer function in the ESRI ArcGIS 9.3 software (Fig. 5).

Landscape metrics selection

In this paper, number of patches, Interspersion and Juxtaposition and percentage of landscape (Table 3) from class level were selected to analyze fragmentation, composition, coherence and dispersion of arable land change trend in FRAGSTATS 3.3 software (McGarigal et al. 2002).

Result and analysis

Spatial and temporal dynamics of arable land in Nanjing metropolitan region

Arable and non-arable land maps in six epochs from 1985 to 2010 were obtained with overall accuracy and Kappa coefficient higher than 85 % and 0.84, respectively. Arable land increased from 1985 to 1990, then decreased dramatically until 2010 (Fig. 2). Arable land decreased by 57.24 % during 1985–2010. Arable land increased by 7.74 % between 1985 and 1990 while it decreased by
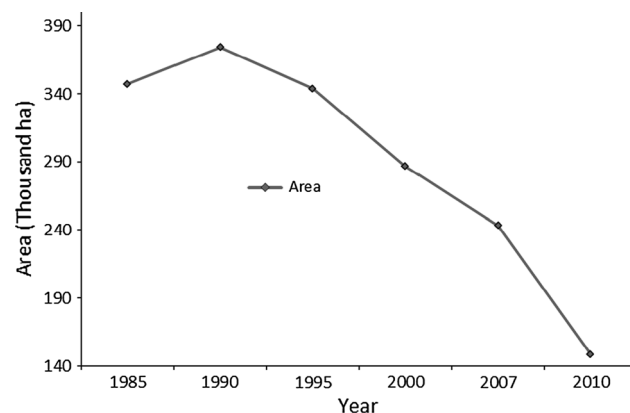
60.31 % from 1990 to 2010. The maximum change magnitude of arable land was 38.93 %, which occurred in the 2007–2010 period.

Spatial distribution of arable land change trajectory

Arable land changes trajectory in various directions

Arable land change trajectory map was extracted based on the arable/non-arable land maps from 1985 to 2010 (Fig. 3). The percentage of five arable land change trajectory types was calculated in eight directions (Table 4). Stable arable land category had the largest proportion (56.89 %) in direction three (North–Northwest, 90°–135°) and the smallest proportion in direction one. Stable non-arable land is mainly dominant in the directions one and three. Change into non-arable land was mainly dominant in the directions one, six, and eight, which revealed the main direction of urban expansion.

Arable land changes trajectory in various counties

Liuhe District had the highest stable arable land (895.92 km²) (Fig. 4). Jiangning District was the second largest with stable arable (696.37 km²) while Jiangnan Districts had smallest stable arable land. Change into non-arable land was the maximum in Jiangning District where numerous arable lands were transformed into construction land. In addition to urbanization, another factor that contributed to the observed arable land loss was construction of aquaculture ponds.

Arable land changes trajectory analysis in various buffers

Stable arable land was mainly concentrated in the area far away from city center of Nanjing with 55.16 % being in the buffer between 25 and 30 km (Fig. 5; Table 5). The percentage of the stable arable land increased with increasing distance from the city center. A complete reverse trend was,


Fig. 2 Changes in arable land area in Nanjing metropolitan region, 1985–2010

Fig. 3 Arable land change
trajectory map
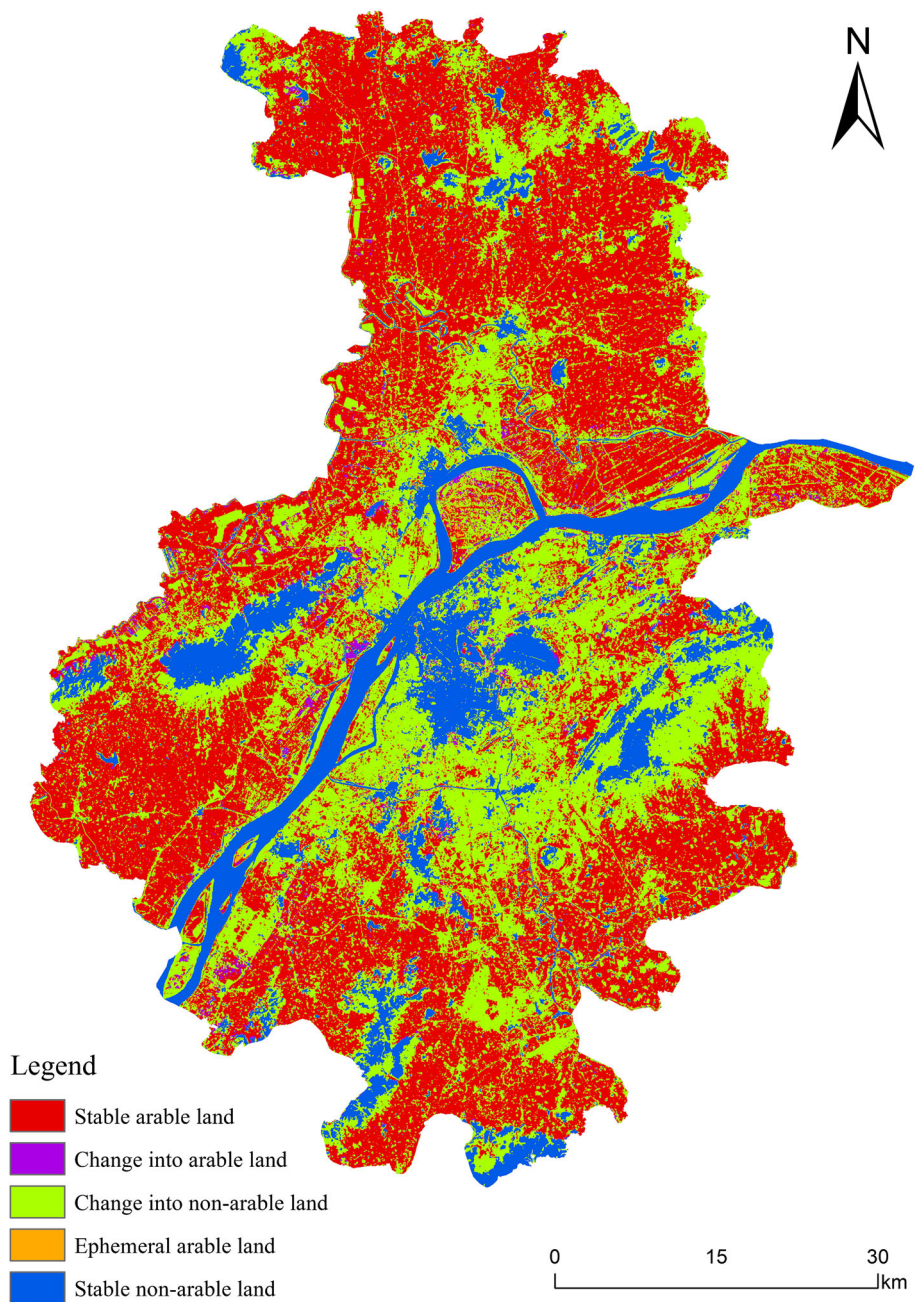
Table 4 Percentage of arable
land change trajectories in eight
directions (%)

|	D1	D2	D3	D4	D5	D6	D7	D8
Stable arable land	26.15	53.37	56.89	34.74	52.71	44.45	44.82	42.12
Change into arable land	2.46	1.70	1.70	4.14	1.32	2.41	0.95	0.60
Change into non-arable land	46.41	34.56	29.61	35.49	30.09	38.39	46.26	44.47
Ephemeral arable land	1.03	0.87	0.72	1.18	0.75	0.86	0.71	0.33
Stable non-arable land	23.95	9.50	11.07	24.45	15.14	13.89	7.25	12.48

however, observed for the non-arable dynamics. The per-
centage of stable non-arable land decreased from 70.3 % in
buffer 0–5 km to 8.745 in buffer 25–30 km. Ephemeral

arable land decreased from 1.97 to 0.77 % with increasing
distance from the city center. The change trend of ephemeral
arable land illustrated that areas nearby the city center

Fig. 4 The area of arable land change trajectories in various counties
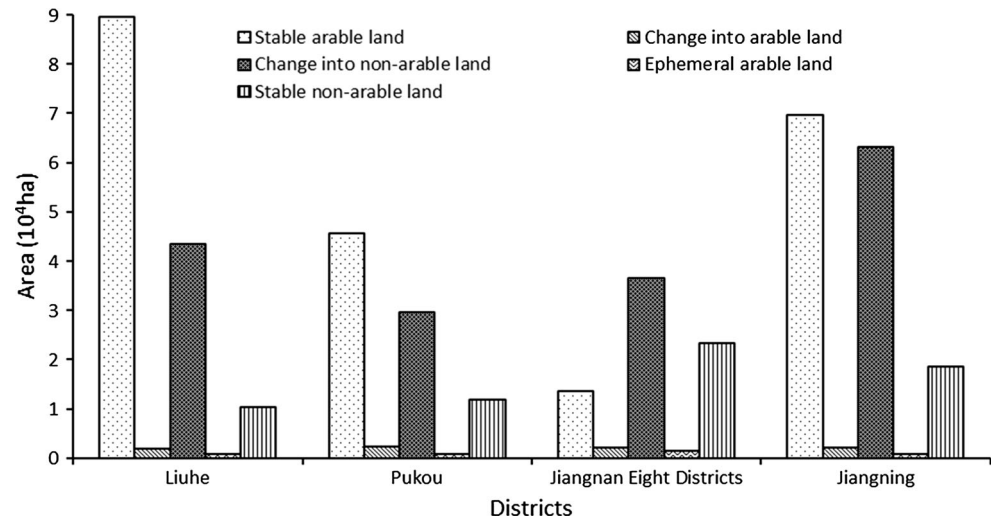
Fig. 5 Distribution of arable land change trajectories in the various buffers
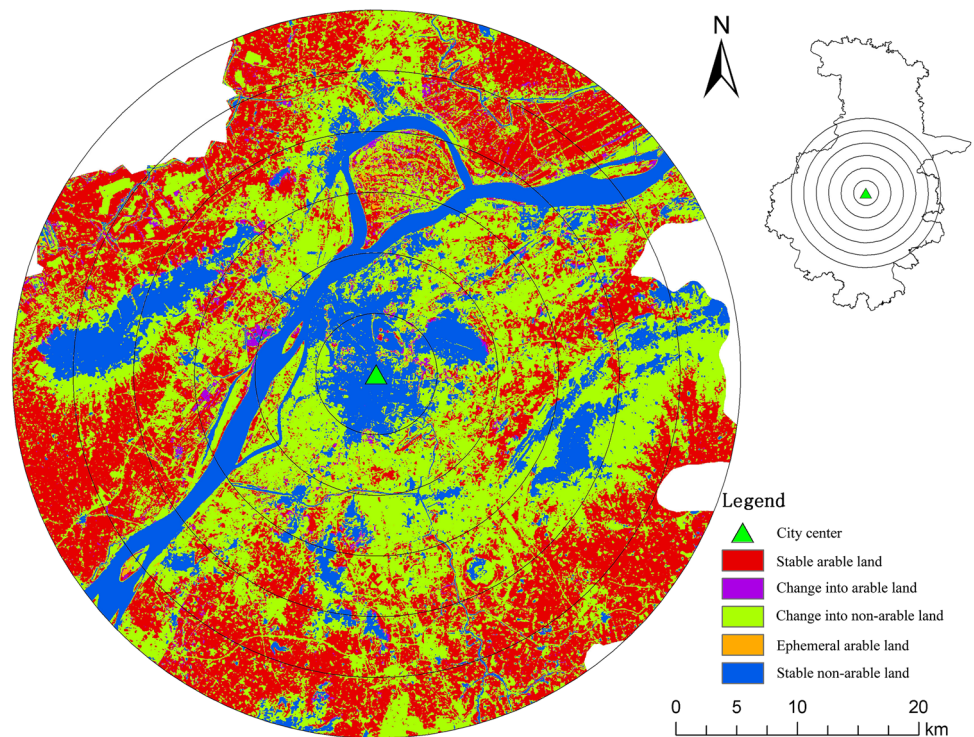
changed dramatically and arable land was the most non-stable. Non-arable land experienced the highest (59.2 %) and the lowest (23.88 %) change within 10–15 km and 0–5 km buffer, respectively. Change into arable land was the lowest (<3 % in six buffers) among the change trend types.

Arable land change trajectory landscape pattern analysis

The percentage of stable arable land was 46.72 %, implying that it constitutes a major land use component in the study area (Table 6). The second largest land cover was

change into non-arable land (36.93 %). The percentage of change into non-arable land revealed sharp reduction of arable land. Stable non-arable land accounted for 13.72 %, including built-up land, water body and forest. Change into arable land and ephemeral arable land accounted for 1.83 and 0.80 %, respectively. The former was caused by land reclaimed due to land policy while the latter was mainly caused by agricultural restructuring.

Interspersion and Juxtaposition (IJI) of stable arable land and stable non-arable land were both less than 35, implying the two types had high spatial association and high stability. Ephemeral arable land had the highest IJI

Table 5 Statistics of arable land change in different buffers

Types	5 km	10 km	15 km	20 km	25 km	30 km
Stable arable land	1.26	7.62	19.47	27.82	44.04	55.16
Change into arable land	2.60	1.97	2.90	2.53	2.04	1.84
Change into non-arable land	23.88	53.91	59.26	49.25	38.75	33.49
Ephemeral arable land	1.97	1.48	1.33	1.19	0.79	0.77
Stable non-arable land	70.30	35.03	17.04	19.21	14.37	8.74

Table 6 Landscape metrics of arable land change trajectories

Types	PLAND	IJI	NP
Stable arable land	46.72	34.89	8,915
Change into arable land	1.83	79.56	14,300
Change into non-arable land	36.93	65.71	20,326
Ephemeral arable land	0.80	80.25	11,676
Stable non-arable land	13.72	32.97	5,950

value (80.25) reflecting the extreme unstable nature of these land cover types. The patch number of change into non-arable land was the largest, indicating high landscape fragmentation associated with conversion of arable land into built-up land as a result of urbanization. Among all the change trend types, stable non-arable land had the lowest patch numbers implying the solidarity nature of the stable non-arable lands.

Driving factors analysis

The changes in arable land were mainly human induced. Rapid economic developments, urban expansion and agricultural restructuring were the main driving forces associated with the observed decreased trends in arable land during 1985–2010. Thus, urbanization, agricultural restructuring, policies and rural labor migration were selected to illustrate the mechanism of arable land changes.

Urbanization

Loss of arable land was associated with increase in build-up areas as a result of urbanization (Zhang et al. 2011). The major urbanization was located in the south of Yangtze River. The southwest and east of Nanjing have been both major urban expansion directions since 1988, especially in Jiangning District (Xu et al. 2007). Urban expansion encroaches the nearby arable lands, which explains the

high instability of arable lands within the vicinity of the center. Land use intensity in the industrial parks and economic development zones was low, which caused loss in high quality arable land. In addition, large numbers of national infrastructures (such as expressway) were developed on arable lands.

Rural labor transformation

Due to economic development, a huge new floating population of rural–urban migrants is transforming the urban labor force in China (Seeborg et al. 2000; Bhattacharyya and Parker 1999). According to the statistical data from National Bureau of Statistics of China (NBSC), the number of rural labors in Nanjing Metropolitan Region has gradually decreased by 49.2 % from 1985 to 2010 (NBSC 2011). In addition, the age structure of rural labor also changed, with increasing trends of large numbers of young labors opting for non-agricultural city jobs. This has had indirect implications on the arable land change dynamics in that arable lands were abandoned due to lack of labor or high cost thereof, giving room for conversion of the land into other land cover uses. A report from the National Bureau of Statistics of China showed that youth laborers between the ages of 26–45 occupied 64.41 % of the total rural labor migration in 2005 (NBSC 2005).

Agricultural restructuring

Driven by variations in the market efficiency of agricultural products (Zhao et al. 2012; Veeck and Pannell 1989), farmers were enticed to transform arable land to aquaculture and orchard. However, this process is unstable and can be sometimes inversed caused by changes in market efficiency, land use and water resource protection policies. This agricultural restructuring has resulted in instability of arable land changes.

Policy-driven factors

Land policy and rural tax reforms and agricultural subsidies have acted to slow down arable land reduction. Chinese Land Management Laws were promulgated and revised twice in 1998 and 2004 to establish land use controlling system. The revised land policies proposed arable land protection (Nanjing Municipal Government 2007). Reforms on rural taxes changed agricultural production distribution income and this increased farmers' income. Agricultural subsidies, such as grain, seed and fertilizer subsidies, improved the comparative advantage of agriculture to increase grain production (Long and Zou 2010).

Conclusions

Detailed arable land change dynamics using the temporal change trajectory approach based on Landsat data was analyzed. Conversion of arable land into non-arable land was mainly dominant within the urban fringes due to rapid urbanization and industrialization. Change into non-arable land was dramatic and characterized by high fragmentation compared to other change trends. Such change trends were attributed to high urbanization. Rural labor migration, economic development, policies and urban expansion are the major driving forces to the observed arable land dynamics.

References

Bhattacharyya A, Parker E (1999) Labor productivity and migration in Chinese agriculture: a stochastic frontier approach. China Econ Rev 10:59–74

Coppin P, Jonckheere I, Nackaerts K, Muys B, Lambin E (2004) Digital change detection methods in ecosystem monitoring: a review. Int J Remote Sens 25:1565–1596

Feng YX, Luo GP, Lu L, Zhou DC, Han QF, Xu WQ, Yin CY, Zhu L, Dai L, Li YZ, CF L (2011) Effects of land use change on landscape pattern of the Manas River watershed in Xinjiang, China. Environ Earth Sci 64:2067–2077

Kuemmerle T, Chaskovskyy O, Knorn J, Radeloff VC, Kruhlov I, Keeton WS, Hostert P (2009) Forest cover change and illegal logging in the Ukrainian Carpathians in the transition period from 1988 to 2007. Remote Sens Environ 113:1194–1207

Lambin EF (1997) Modeling and monitoring land cover change processes in tropical regions. Prog Phys Geog 21:375–393

Liu XH, Wang JF, Liu ML, Meng B (2005a) Arable land change and driving forces analysis in China. China Sci Ser D Earth Sci 35:1087–1095

Liu JY, Liu ML, Tian HQ, Zhuang DF, Zhang ZX, Zhang W, Tang XM, Deng XZ (2005b) Spatial and temporal patterns of China's cropland during 1990–2000: an analysis based on Landsat^{TM} data. Remote Sens Environ 98:442–456

Liu GL, Zhang LC, Zhang Q, Musyimi Z, Jiang QH (2014a) Spatio–temporal dynamics of wetland landscape patterns based on remote sensing in Yellow River Delta, China. Wetlands 34:787–801

Liu GL, Kurban A, Duan HM, Umit H, Abdimijt A, Zhang LC (2014b) Desert riparian forest colonization in the lower reaches of Tarim River based on remote sensing analysis. Environ Earth Sci 71:4579–4589

Liu GL, Zhang LC, Zhang Q, Musyimi Z (2014c) The response of grain production to changes in quantity and quality of cropland in Yangtze River Delta, China. J Sci Food Agric. doi:10.1002/jsfa.6745

Long HL, Liu YS, Wu XQ, Dong GH (2009) Spatio-temporal dynamic patterns of farmland and rural settlements in Su-Xi-Chang region: implications for building a new countryside in coastal China. Land Use Pol 26:322–333

Long HL, Zou J (2010) Grain production driven by variations in farmland use in China: an analysis of security patterns. J Resour Ecol 1:60–67

Lu D, Mausel P, Brondízio E, Moran E (2004) Change detection techniques. Int J Remote Sens 25:2365–2407

Markham BL, Barker JL (1987) Radiometric properties of US processed Landsat MSS data. Remote Sens Environ 22:39–71

McGarigal K, Cushman SA, Neel MC, Ene E (2002) FRAGSTATS v3: spatial pattern analysis program for categorical maps. Computer software program produced by the authors at the University of Massachusetts, Amherst

Moran MS, Jackson RD, Slater PN, Teilet PM (1992) Evaluation of simplified procedures for retrieval of land surface reflectance factors from satellite sensor output. Remote Sens Environ 4:169–184

Nanjing Municipal Government (2007) Suggestions about strengthening primary farmland protection and management in Nanjing. http://www.njgt.gov.cn/default.php?mod=article&do=detail&tid=208891

NBSC (2005) The rate of suburban rural labor migration is nearly two-thirds in Nanjing. http://news.cnfol.com/050802/101,1281,1371385,00.shtml

NBSC (2011) Nanjing statistical yearbook in 2011. China Statistical Yearbook Press, Beijing

Ouyang XJ, Lou Q, Gu LB (2012) Cardiovascular disease risk factors are highly prevalent in the office-working population of Nanjing in China. Int J Cardiol 155:212–216

Price JC (1987) Special issue on radiometric calibration of satellite data. Remote Sens Environ 22:1–158

Seeborg MC, Jin ZH, Zhu YP (2000) The new rural–urban labor mobility in China: causes and implications. J Socio Econ 29:39–56

Shi B, Tang CS, Gao L, Liu C, Wang BJ (2012) Observation and analysis of the urban heat island effect on soil in Nanjing, China. Environ Earth Sci 67:215–229

Turner HBL, Skole D, Sanderson S (1995) Land-use and land-cover change science/research plan. IGBP Report No.35 and HDP Report No.7, Stochkholm, IGBP

Turner BL II, Matson PA, McCarthy JJ, Corell RW, Christensen L, Eckley N, Hovelsrud-Broda GK, Kasperson JX, Kasperson RE, Luers A, Martello ML, Mathiesen S, Naylor R, Polsky C, Pulsipher A, Schiller A, Selin H, Tyler N (2003) Illustrating the coupled human-environment system for vulnerability analysis: three case studies. PANS 100:8080–8085

Veeck G, Pannell CW (1989) Rural economic restructuring and farm household income in Jiangsu, People's Republic of China. Ann Assoc Am Geogr 79:275–292

Wang DC, Gong JH, Chen LD, Zhang LH, Song YQ, Yue YJ (2012) Spatio-temporal pattern analysis of land use/cover change trajectories in Xihe watershed. Int J Appl Earth OBS 14:12–21

Xu C, Liu MS, Zhang C, An SQ, Yu W, Chen JM (2007) The spatiotemporal dynamics of rapid urban growth in the Nanjing metropolitan region of China. Landsc Ecol 22:925–937

Xu C, Liu MS, Yang XJ, Sheng S, Zhang MJ, Huang Z (2010) Detecting the spatial differentiation in settlement change rates during rapid urbanization in the Nanjing metropolitan region, China. Environ Monit Assess 171:457–470

Zhang HY, Uwasu M, Hara K, Yabar H (2011) Sustainable Urban development and land use change—a case study of the Yangtze River Delta in China. Sustainability 3:1074–1089

Zhao YL, Li XB, Xin LJ, Hao HG (2012) Geographic concentration and driving forces of agricultural land use in China. Front Earth Sci 6:48–56

Zhou QM, Li BL, Kurban A (2008a) Trajectory analysis of land cover change in arid environment of China. Int J Remote Sens 29:1093–1107

Zhou QM, Li BL, Kurban A (2008b) Spatial pattern analysis of land cover change trajectories in Tarim Basin, northwest China. Int J Remote Sens 29:5495–5509